Catalysis Today 175 (2011) 78–82

Contents lists available at ScienceDirect

Catalysis Today

journal homepage: www.elsevier.com/locate/cattod

Effect of reductive treatments on Pt behavior and NO_x storage in lean NO_x trap catalysts

XianQin Wang[1], Do Heui Kim*, Ja Hun Kwak, Chongmin Wang, Janos Szanyi, Charles H.F. Peden**

Institute for Interfacial Catalysis, Pacific Northwest National Laboratory, P.O. Box 999, Richland, WA 99352, USA

ARTICLE INFO

Article history:
Received 1 November 2010
Received in revised form 1 March 2011
Accepted 14 March 2011
Available online 27 April 2011

Keywords:
Lean NO_x traps
Reducing temperatures
Ba migration

ABSTRACT

Lean NO_x trap (LNT) catalysts represent a promising approach to meet increasingly stringent NO_x emission regulations on diesel and other lean-burn engines. Pt material properties, including dispersion and particle size, are known to be important factors in determining NO_x uptake performance, since Pt provides active sites for NO oxidation to NO_2 necessary for storing NO_x as nitrates, and for the reduction of nitrates to N_2. In this work, the physicochemical properties of Pt in Pt–BaO/Al_2O_3 LNT catalysts, such as the Pt accessible surface area and particle size, were investigated by using various tools, such as irreversible volumetric H_2 chemisorption, high resolution transmission electron microscopy (HRTEM), and X-ray diffraction (XRD), following successive reductive treatments at elevated temperatures. NO_x uptake activities were also measured to establish a relationship between the properties of Pt and NO_x storage following identical high-temperature reductive treatments. We find that the reductive treatments of Pt–BaO/Al_2O_3 lean NO_x trap catalysts at temperatures up to 500 °C promote a significant increase in NO_x uptake explained, in part, by an induced close interaction between Pt and BaO phases in the catalyst, thus enabling facilitation of the NO_x storage process.

1. Introduction

The lean NO_x trap (LNT) technology [1,2] is considered as one of the after-treatment solutions to reduce NO_x emissions from lean burn or diesel engines, those that operate under highly oxidizing conditions. Typically, LNT catalysts (also known as NO_x storage reduction (NSR) catalysts or NO_x adsorbers) usually consisting of precious metals (e.g. Pt and Rh), a storage element (BaO) and a high surface area support material (e.g. Al_2O_3), operate under transient conditions that include lean and rich phases [3]. With continuing research regarding NO_x storage and regeneration steps, the overall mechanism over LNT catalyst is relatively well understood [4–10].

Platinum plays critical roles in various steps of the NO_x storage and reduction process. First, Pt catalyzes the oxidation of NO to NO_2, which is subsequently stored as nitrates by barium components during lean conditions. In addition, Pt is actively involved in the reduction of the released NO_x under rich conditions [11]. Olsson and Fridell [12] reported that NO oxidation rates decrease with increasing Pt dispersion, attributed to the formation of less active PtO for small Pt particles, although the highest NO_x uptakes were obtained for samples with the highest Pt dispersions [13].

With regard to the specific NO_x storage mechanism during complete uptake, Epling et al. [14,15] suggest the presence of two different Ba sites depending on their proximity to Pt, such that the Ba sites close to Pt store NO_2 more readily during a full NO_x uptake period, while the Ba sites far from Pt store NO_2 via a disproportionation mechanism. Furthermore, in NO_x uptake experiments with varying NO concentrations [10], it was found that the efficiency of barium in storing NO_x was proportional to NO concentration, which led to the proposal that the primary route for NO_x storage is a 'spillover' of NO_2 from Pt to neighboring barium sites. Buchel et al. [16] also reported on a beneficial role for close interactions between Pt and Ba during the NO_x storage step. These results underline the importance of neighboring barium sites adjacent to Pt sites; in other words, intimate interaction between Pt and barium.

Thus, a next question arises about how to enhance interactions between Pt and barium. In this study, promotion of such interactions between Pt and barium to improve the NO_x uptake performance, via conditions known to lead to so-called strong metal–support interactions (SMSI), was explored [17,18]. Tauster et al. [19] the first described such SMSI phenomena for Pt/TiO_2 catalysts, where the amount of CO or H_2 chemisorbed on Pt significantly decreased as a result of a high-temperature reduction step with H_2. The decrease in the amount of chemisorbed H_2 on is the Pt was explained by decreased reduced accessible metal surface area

* Corresponding author. Tel.: +1 509 371 6489.
** Corresponding author. Tel: +1 509 371 6501.
E-mail addresses: do.kim@pnl.gov (D.H. Kim), chuck.peden@pnl.gov (C.H.F. Peden).
[1] Current address: Otto H. York Department of Chemical, Biological and Pharmaceutical Engineering, New Jersey Institute of Technology, Newark, NJ 07102, USA.

0920-5861/$ – see front matter © 2011 Published by Elsevier B.V.
doi:10.1016/j.cattod.2011.03.032

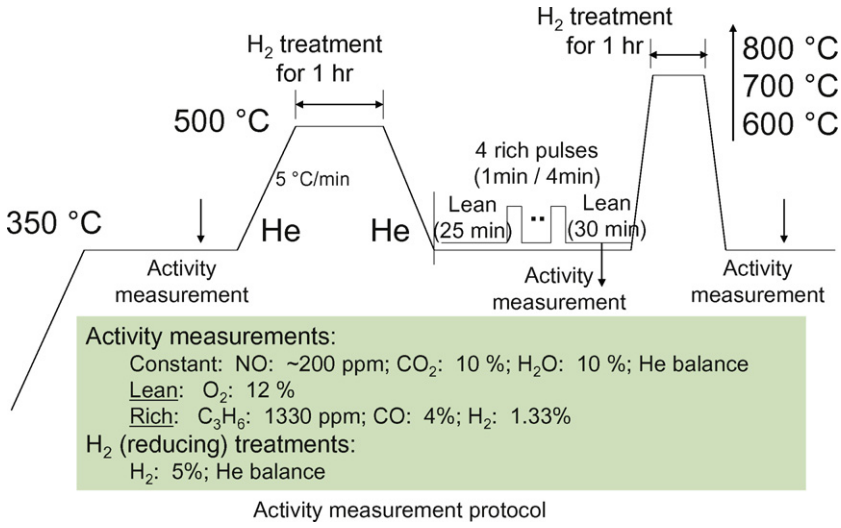

Fig. 1. Reaction protocol used for the NO_x uptake measurements performed in this study.

resulting from encapsulation of the Pt particles by a thin sub-oxide layer from the support, thus promoting interactions between the Pt and the TiO_2 support material. This induced interaction changes the performance of these catalysts [20].

In this contribution, we explore the possibility that similar high-temperature reduction treatments can lead to enhancements in the interactions between Pt and Ba, and investigate the relationship between Pt behavior and the NO_x uptake performance as a function of reduction temperatures. In particular, the behavior of Pt, including Pt accessibility and Pt particle size, is studied by means of irreversible volumetric H_2 chemisorption, high-resolution transmission electron microscopy (TEM), and X-ray diffraction (XRD) techniques.

2. Experimental

2.1. Materials

An LNT catalyst sample of Pt (1.5 wt%)–BaO (16%)/Al_2O_3 in a powder form was supplied by the Johnson Matthey Company (Wayne, PA). The sample was first calcined with a 10% O_2/He gas mixture at 500 °C for 2 h, and then treated in H_2 for 2 h at various temperatures prior to the H/Pt and NO_x uptake measurements.

2.2. H/Pt measurements

Platinum accessibility was evaluated via the irreversible H_2 chemisorption method in order to estimate the number of hydrogen atoms per Pt (H/Pt). These measurements were performed in a static mode at room temperature using a conventional volumetric apparatus. Typically, 0.5 g of catalyst was dried and used. Before the H_2 chemisorption measurements, the catalyst was first reduced in H_2 (30 sccm) at 300 °C for 2 h with subsequent evacuation at 400 °C for an additional 2 h. Then, the sample was cooled down under vacuum to 20 °C. Two hydrogen adsorption isotherm curves were obtained, followed by expansion coefficient measurements and evacuation. After the first isotherm, the catalyst was evacuated again for 1 h. The amount of total and reversible hydrogen uptakes were then estimated by extrapolating the quasi-linear portions of the isotherm to zero pressure. The difference between these two values gave the amount of irreversible hydrogen uptake, from which the number of accessible metallic atoms (designated as H/Pt) was calculated assuming a stoichiometry of 1 hydrogen atom per surface metal atom [21]. Using the same sample, H/Pts were then consecutively obtained following high-temperature (400, 500, 600, 700, 800 °C) reduction using the same protocol as above. After finishing the H/Pt measurement for the sample reduced at 800 °C, the sample was oxidized in dry air at 400 °C for 1 h and re-reduced at 300 °C, and then H/Pt was measured protocol final time.

2.3. High-resolution TEM and XRD

The morphology of the samples after various treatments was characterized with high resolution TEM. The TEM specimens were prepared by dispersing fine catalyst powder particles onto a carbon film coated 200 mesh copper TEM grid. TEM analysis was carried out on a JEOL JEM 2010 microscope with a specified point-to-point resolution of 0.194 nm. The operating voltage of the microscope was 200 keV. All images were digitally recorded with a slow scan CCD camera (image size 1024 × 1024 pixels), and image processing was carried out using a Digital Micrograph (Gatan). The composition of the particles was analyzed by energy-dispersive X-ray spectroscopy (EDS). The EDS spectrometer is an Oxford Link system attached onto the transmission electron microscope.

X-ray diffraction patterns of the samples after the reduction at 800 °C were collected with a Philips X'Pert MPD system. The X-ray source is a long-fine-focus, ceramic X-ray tube with a Cu anode. Normal operating power is 40 kV and 50 mA (2.0 kW).

2.4. NO_x uptake measurements

LNT performance was evaluated in a fixed bed quartz reactor operated under continuous lean-rich cycling using 0.117 g of catalyst. NO_x concentrations in the inlet and outlet gases were measured with a chemiluminescence NO_x analyzer (Thermo Electron, 42C). NO_x uptake (%) was defined as the ratio of the amount of adsorbed NO_x to the amount of inlet NO_x integrated over 30 min. Reactants consisted of a continuous flow of 200 ppm NO, 10% CO_2 and 10% H_2O balanced with He, with either a rich (1330 ppm C_3H_6, 4% CO and 1.33% H_2) or lean (12% O_2) gas mixture added. All of the gases were controlled by mass flow controllers (Brooks), and NO_x storage performance was measured at 350 °C. The reaction protocol for these NO_x uptake measurements is illustrated in Fig. 1. Initially, four sequences of 1 min rich and 4 min lean cycles were introduced at 350 °C, and NO_x uptake was measured during a lean period for 30 min after 4th pulse (first descending vertical arrow in Fig. 1). Very similar to the H/Pt measurements, successive reducing treatments at elevated temperatures (from 500 to 800 °C) were then

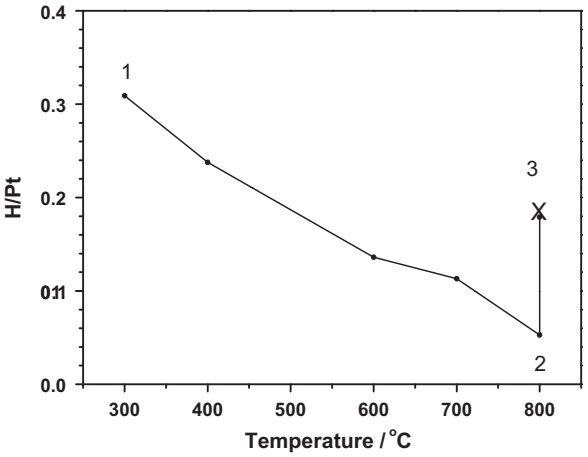

Fig. 2. H/Pt ratios obtained from H_2 chemisorption measurements for Pt–BaO/Al_2O_3 samples after reduction at elevated temperatures from 300 to 800 °C.

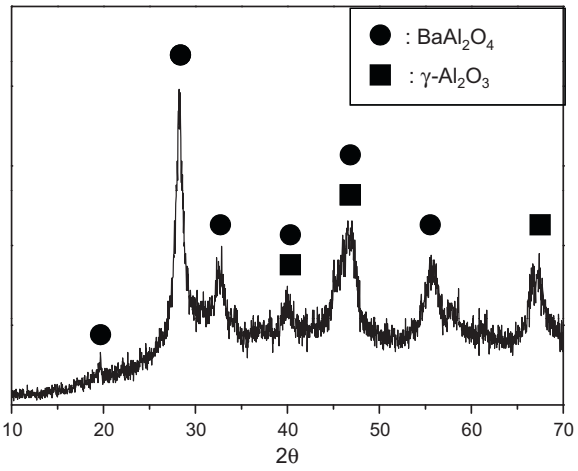

Fig. 3. XRD pattern for the Pt–BaO/Al_2O_3 sample after reduction at 800 °C.

applied to the samples, with NO_x uptake measurements after each reduction treatment (second and third descending vertical arrows in Fig. 1). A 5% H_2/He gas mixture was applied for 1 h at the desired temperature during the reducing treatments.

3. Results and discussion

H/Pt values determined from H_2 chemisorption measurements are regarded as the accessible surface area of Pt in supported Pt catalysts. Fig. 2 shows the change of H/Pt values acquired for the LNT sample used here after successive reducing treatments at each temperature. There is an apparent trend that the H/Pt ratio decreases monotonically with increasing reduction temperature.

Initially, we focused on the behavior of Pt at two reduction temperatures, marked as 1 and 2 in Fig. 2, with large differences in H/Pt values representing LNT model catalysts after reduction at 300 and 800 °C, respectively. Based on the calculation that assumes spherical Pt particles [22], the estimated sizes of Pt particles at 1 and 2 are 4 nm and 26 nm, respectively, as also listed in the third column in Table 1. Clearly, these H_2 chemisorption results suggest that Pt particles grow significantly in size during reduction up to 800 °C. Such a change might be explained by sintering at 800 °C, since it is widely known that Pt species can become mobile above 600 °C to form larger particles [23]. However, it must be pointed out that the estimated Pt size of 26 nm is much larger than that observed for a reduced Pt–BaO/Al_2O_3 sample at 990 °C for 5 h, which gave rise to an XRD- and TEM-estimated growth of Pt up to just 10 nm [24].

To compare estimated Pt size by H_2 chemisorption with other techniques, we applied XRD to the reduced sample at 800 °C (point 2). As shown in Fig. 3, the XRD pattern of this sample clearly demonstrates the formation of a $BaAl_2O_4$ phase, commonly observed for Pt–BaO/Al_2O_3 LNT catalysts after high temperature reduction [25], in addition to the support γ-Al_2O_3 phase. However, no sharp Pt peak at 2θ of 39.6° is present, implying that the actual crystalline particle size of Pt should actually be less than 10 nm, the detection limit of XRD. Thus, there is a significant discrepancy in the Pt particle size estimates for the sample reduced at 800 °C between the H_2 chemisorptions and XRD measurements.

Table 1
H/Pt ratios and Pt particle sizes estimated from the H/Pt ratios, and from the TEM results for data points 1, 2 and 3 in Fig. 2.

Data points	H/Pt	Particle size from H/Pt (nm)	Particle size from TEM (nm)
1	0.31	4	2–5
2	0.05	26	5–10
3	0.18	7	5–10

To reconcile this discrepancy, high-resolution TEM images for the two samples (points 1 and 2) were obtained and are shown in Fig. 4(a) and (b), respectively. The Pt particle sizes after these various treatments did not vary significantly unlike the estimates from the H/Pt values. The Pt particle sizes, estimated from these TEM images (listed in the last column in Table 1) for samples 1 and 2 are 2–5 nm and 5–10 nm, respectively, which is consistent with the XRD results. Thus, both XRD and TEM results give Pt particle sizes of 5–10 nm, while estimates from H/Pt measurements suggest much larger values of 26 nm for the sample reduced at 800 °C.

On the basis of these results and in analogy with prior conclusions about SMSI-like phenomena [26], we suggest that the decrease in H/Pt arises primarily from the covering of Pt surfaces with Ba species, induced by the reduction step, and not from Pt sintering due to the thermal aging. Due to such an encapsulation process, with increasing the reduction temperature the accessible Pt area for H_2 chemisorption monotonically decreases, while the average Pt size grows only marginally from 2–5 nm to 5–10 nm. In other words, the reduction treatments lead to mobile Ba species that migrate to the surface of Pt, resulting in a more intimate interaction between Pt and Ba.

In support of this proposal about the migration of Ba species to the surface of Pt, subsequent oxidation of the 800 °C reduced sample induces a significant increase in the H/Pt ratios (from 0.05 to 0.18), as evidenced by point 3 in Fig. 2, obtained following subsequent O_2 treatment at 400 °C. Note that a H/Pt ratio of 0.18 corresponds to a Pt particle size of 8–10 nm according to the Shere equation [22]. As demonstrated in the TEM images in Fig. 4(b) and (c), there is not much difference in Pt particle size; both images before and after oxidation demonstrate the Pt particles ranging from 5 to 10 nm. Thus, this change in H/Pt ratios induced by subsequent O_2 treatment can be understood as arising from the reversible transfer of barium species from Pt surface and, again, not due to Pt particle size change.

It can be summarized that the reductive treatment up to 800 °C gives rise to a very modest growth of Pt particles (from 2–5 nm to 5–10 nm by TEM) and formation of a $BaAl_2O_4$ phase (by XRD). However, the large decrease in Pt accessible area, measured by H_2 chemisorption, does not originate from the sintering of Pt, but primarily from partial covering of the Pt surface with Ba. The location of mobile barium is reversible depending on the gas environment; H_2 reduction induces the partial encapsulation of Pt by Ba while oxidation by O_2 results in Ba migration away from Pt surface. In

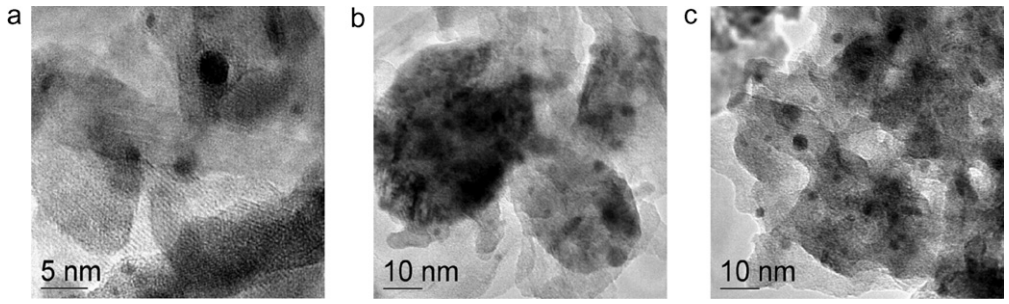

Fig. 4. TEM images for Pt–BaO/Al_2O_3: (a) after reduction at 300 °C; (b) after reduction at 800 °C; and (c) after re-oxidation at 400 °C following reduction at 800 °C.

view of these conclusions, we next considered whether the close interaction induced by Ba migration affected the NO_x uptake performance. In order to address this critical question for the LNT material, we measured NO_x uptake activity over the Pt/Ba–Al_2O_3 catalyst following reduction with 10% H_2/He for 1 h at different temperatures; essentially the same procedure performed prior to the H/Pt measurements.

NO_x uptakes were measured sequentially for samples reduced at 500, 600, 700 and 800 °C, in addition to a fresh Pt–Ba/Al_2O_3 sample without reduction. Note that an experimental difference between H/Pt and NO_x uptake measurements is that, in the latter, samples are exposed to lean conditions at NO_x uptake performance temperature of 350 °C following reduction at desired temperature (see Fig. 1). Fig. 5 displays the original NO_x uptake curves after a 1 min rich pulse of the 4th lean/rich cycle for (lean NO_x uptake begins around 980 s). Most interesting is the significant increase in overall NO_x uptake relative to a fresh sample after reduction at 500 °C; especially note the longer complete NO_x uptake period. The activity results demonstrate that the reducing treatment has significantly promoted the NO_x uptake process. On the other hand, further increases in the reduction temperature from 500 to 800 °C results in a decrease in NO_x uptakes. Note, however, that, except for the sample reduced at 800 °C, NO_x uptakes for reduced samples are still larger than those of the fresh sample. This observation is more clearly demonstrated in Fig. 6 which plots (dashed lines) NO_x uptakes (%) determined after 30 min lean uptake. In this figure, point *a* represents the NO_x uptake (%) from the fresh sample without a prior reduction treatment, while point *b* is from the sample reduced at 350 °C (original curve not shown in Fig. 5). By comparing these two points, it is clear that the sample reduced at 350 °C has a much larger NO_x uptake relative to the fresh one. This result again suggests a possible importance for close interaction between Pt and Ba in the LNT materials, created even at a relatively low reduction temperature.

In order to better define the possible relationship between Pt/Ba interactions and the performance of the LNTs, we plot both the NO_x uptake and the H/Pt values with respect to the reduction temperature in Fig. 6. There it can be clearly seen that, while the NO_x uptake has a maximum value after 500 °C reduction, H/Pt values monotonically decreased with the increase in the reduction temperature as described earlier. We discuss these comparative results in two different regions (A and B) as marked in Fig. 6. In region A, NO_x uptake actually increases, in contrast to the decreasing accessible Pt surface area. In particular, increases in the reduction temperature from 350 to 500 °C give rise to NO_x uptakes that are significantly larger (by about 25%) while Pt accessible surface area decreases by as much as 40%. As suggested earlier, a possible explanation for this result may be that an enhanced Pt–Ba interaction, induced after reduction at 500 °C, could make BaO more reactive for NO_x uptake than those BaO species in the sample reduced at 350 °C. In particular, the reduction treatment might result in a redistribution of Ba species towards Pt such that the intrinsic NO_x uptake of the Ba species is enhanced through more efficient use of Ba in the catalyst. Such an explanation is consistent with previous studies [16] that identified enhanced proximity between Pt and BaO via synthesis using a two-nozzle flame spray pyrolysis method. Catalysts prepared in this way gave rise to higher NO_x uptakes than those prepared by conventional impregnation.

In the highlighted region B in Fig. 6, where reduction temperatures exceed 600 °C, there are possibly multiple factors that contribute to the observed decrease in the NO_x uptakes. Within this temperature range, Pt particle sizes slightly increase to 5–10 nm range from a 2–5 nm range, and a significant amount of $BaAl_2O_4$ is formed. Such thermal aging processes are known to have a negative

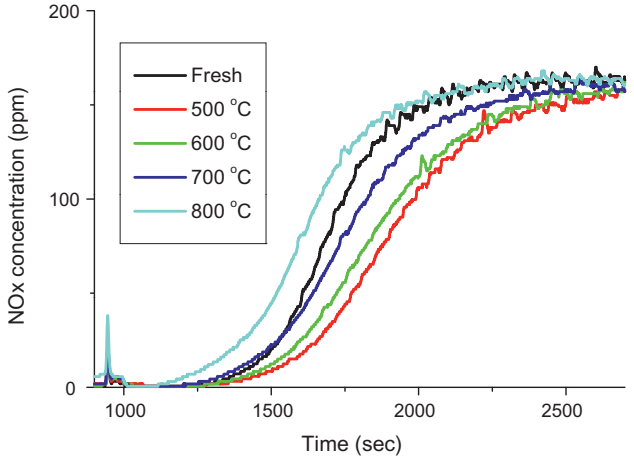

Fig. 5. NO_x uptake curves after for a fresh sample, and for samples after reducing treatment at various temperatures.

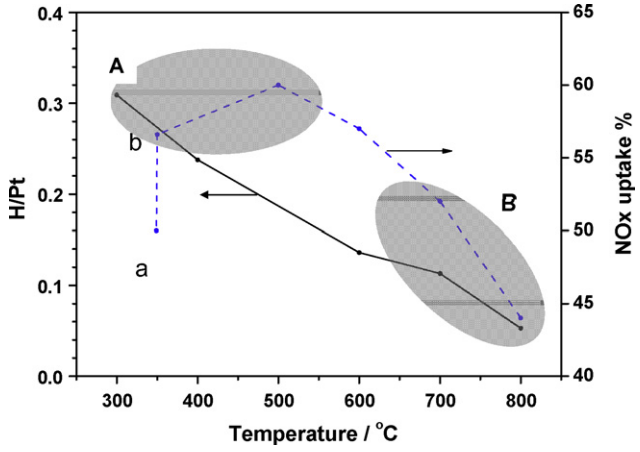

Fig. 6. Changes of H/Pt ratios and NO_x uptakes (%) as a function of reduction temperature.

effect on the NO_x uptakes. Such processes, however, are non-linear, becoming especially problematic above a threshold temperature [27]. As such, Pt size growth and Ba phase changes cannot explain the somewhat monotonic decrease in NO_x uptakes above 500 °C reduction temperatures. Instead, we suggest that, while Ba migration that enhances Pt/Ba interactions is beneficial, an increasing loss of accessible Pt surface area (as evidenced by the continuous drop in H/Pt ratios) eventually overrides the positive effects of this migration.

In support of these conclusions, recall the H_2 chemisorption results in Fig. 2 which showed that H/Pt ratios significantly increased after an oxidation treatment of the high-temperature (800 °C) reduced sample. Consistent with prior understanding of SMSI effects [26], higher H/Pt values after re-oxidation of a high-temperature reduced catalyst represents a re-opening of accessible Pt surface area. Thus, the aggregate of the H_2 chemisorption, XRD and TEM results indicate a migration of barium species towards and away from Pt during elevated temperature reduction and oxidation. These processes can induce a beneficial enhancement of Pt/Ba interactions but also a decrease in accessible Pt surface area that can be detrimental to the LNT catalyst performance.

4. Conclusions

We investigated the physicochemical properties of Pt species, such as the Pt accessible area and Pt particle size, in $Pt/BaO–Al_2O_3$ catalysts and correlated these with measured NO_x uptakes after the successive reductive treatments at elevated temperatures. We find that reductive treatments of $Pt–BaO/Al_2O_3$ lean NO_x trap catalysts at temperatures up to 500 °C promote a significant increase in NO_x uptake, explained, in part, by an induced close interaction between Pt and BaO phases in the catalyst, thus improving the efficient use of barium species in the NO_x storage process. However, the reducing treatment at higher temperature than 500 °C had a negative effect on NO_x storage partly due to loss of accessible Pt surface area and, at the highest reduction temperatures, Pt sintering and $BaAl_2O_4$ formation.

Acknowledgements

Financial support was provided by the U.S. Department of Energy (DOE), Office of Freedom Car and Vehicle Technologies. We also acknowledge valuable discussions with our colleagues at Cummins, Inc. and Johnson Matthey Catalysts. The work was performed in the Environmental Molecular Sciences Laboratory (EMSL) at Pacific Northwest National Laboratory (PNNL). The EMSL is a national scientific user facility and supported by the U.S. Department of Energy (DOE), Office of Biological and Environmental Research. PNNL is a multi-program national laboratory operated for the U.S. DOE by Battelle Memorial Institute under Contract DE-AC06-76RLO 1830.

References

[1] W.S. Epling, L.E. Campbell, A. Yezerets, N.W. Currier, J.E. Parks, Catalysis Reviews-Science and Engineering 46 (2004) 163–245.
[2] S. Roy, A. Baiker, Chemical Reviews 109 (2009) 4054–4091.
[3] N. Takahashi, H. Shinjoh, T. Iijima, T. Suzuki, K. Yamazaki, K. Yokota, H. Suzuki, N. Miyoshi, S. Matsumoto, T. Tanizawa, T. Tanaka, S. Tateishi, K. Kasahara, Catalysis Today 27 (1996) 63–69.
[4] E. Fridell, H. Persson, B. Westerberg, L. Olsson, M. Skoglundh, Catalysis Letters 66 (2000) 71–74.
[5] F. Prinetto, G. Ghiotti, I. Nova, L. Lietti, E. Tronconi, P. Forzatti, Journal of Physical Chemistry B 105 (2001) 12732–12745.
[6] Z.Q. Liu, J.A. Anderson, Journal of Catalysis 228 (2004) 243–253.
[7] J. Szanyi, J.H. Kwak, J. Hanson, C.M. Wang, T. Szailer, C.H.F. Peden, Journal of Physical Chemistry B 109 (2005) 7339–7344.
[8] J. Szanyi, J.H. Kwak, D.H. Kim, S.D. Burton, C.H.F. Peden, Journal of Physical Chemistry B 109 (2005) 27–29.
[9] Y. Su, M.D. Amiridis, Catalysis Today 96 (2004) 31–41.
[10] J.H. Kwak, D.H. Kim, T. Szailer, C.H.F. Peden, J. Szanyi, Catalysis Letters 111 (2006) 119–126.
[11] I. Nova, L. Lietti, L. Castoldi, E. Tronconi, P. Forzatti, Journal of Catalysis 239 (2006) 244–254.
[12] L. Olsson, E. Fridell, Journal of Catalysis 210 (2002) 340–353.
[13] J. Dawody, M. Skoglundh, S. Wall, E. Fridell, Journal of Molecular Catalysis A: Chemical 225 (2005) 259–269.
[14] W.S. Epling, J.E. Parks, G.C. Campbell, A. Yezerets, N.W. Currier, L.E. Campbell, Catalysis Today 96 (2004) 21–30.
[15] W.S. Epling, G.C. Campbell, J.E. Parks, Catalysis Letters 90 (2003) 45–56.
[16] R. Buchel, R. Strobel, F. Krumeich, A. Baiker, S.E. Pratsinis, Journal of Catalysis 261 (2009) 201–207.
[17] D.W. Goodman, Catalysis Letters 99 (2005) 1–4.
[18] Q. Fu, T. Wagner, Surface Science Reports 62 (2007) 431–498.
[19] S.J. Tauster, S.C. Fung, R.L. Garten, Journal of the American Chemical Society 100 (1978) 170–175.
[20] C. Ocal, S. Ferrer, Journal of Chemical Physics 84 (1986) 6474–6478.
[21] E. Rogemond, N. Essayem, R. Frety, V. Perrichon, M. Primet, M. Chevrier, C. Gauthier, F. Mathis, Catalysis Today 29 (1996) 83–87.
[22] S.E. Golunski, H.A. Hatcher, R.R. Rajaram, T.J. Truex, Applied Catalysis B: Environmental 5 (1995) 367–376.
[23] A.K. Datye, Q. Xu, K.C. Kharas, J.M. McCarty, Catalysis Today 111 (2006) 59.
[24] D.H. Kim, Y.H. Chin, J.H. Kwak, C.H.F. Peden, Catalysis Letters 124 (2008) 39–45.
[25] A. Amberntsson, M. Skoglundh, S. Ljungstrom, E. Fridell, Journal of Catalysis 217 (2003) 253–263.
[26] H. Abdulhamid, E. Fridell, J. Dawody, M. Skoglundh, Journal of Catalysis 241 (2006) 200–210.
[27] C.H. Bartholomew, Applied Catalysis A: General 212 (2001) 17–60.